Studies of Inhibitor Binding to *Escherichia coli* Purine Nucleoside Phosphorylase Using the Transferred Nuclear Overhauser Effect and Rotating-Frame Nuclear Overhauser Enhancement

Michael E. Perlman,[†,§] Donald G. Davis,[‡] George W. Koszalka,[∥] Joel V. Tuttle,[∥] and Robert E. London*[,‡]

Laboratory of Molecular Biophysics, National Institute of Environmental Health Sciences, National Institutes of Health, Research Triangle Park, North Carolina 27709, and Division of Experimental Therapy, Wellcome Research Laboratories, Research Triangle Park, North Carolina 27709

Received November 23, 1993; Revised Manuscript Received April 20, 1994[⊕]

ABSTRACT: NMR studies of the adenosine analog tubercidin have been carried out in the presence of *Escherichia coli* purine nucleoside phosphorylase (PNP) in order to characterize the conformation of the enzyme-complexed nucleoside. Although analysis of transferred NOE data at various enzyme/inhibitor ratios indicated a predominantly *syn* nucleoside conformation in the enzyme-complexed state, the results, particularly the 8{1′} and 8{3′} NOE interactions, were not quantitatively consistent with any single bound conformation. Dissociation rate constants for the tubercidin–PNP complex were determined based on analysis of chemical shift and line width data as a function of enzyme/inhibitor ratio, Carr–Purcell–Meiboom–Gill measurements of the transverse relaxation rate as a function of pulse rate, and $T_{1\rho}$ experiments as a function of the spin-lock field strength. Dissociation rate constants of 2100 s^{-1} at 20 °C and 1400 s^{-1} at 10 °C were determined using the latter two methods. These rates are sufficiently high to justify the validity of the transferred NOE method for an enzyme as large as PNP. The possible significance of spin diffusion was investigated by the use of the deuterated analog [2′-^{2}H]tubercidin, for which many of the intraligand spin diffusion pathways are eliminated, and by performing a series of transferred ROE experiments. A comparison of data obtained using transferred NOE and ROE measurements provides a basis for separating direct and indirect relaxation pathways. Both approaches indicated that the relatively significant 8{3′} NOE interaction was not dominated by spin diffusion. Furthermore, analysis of chemical shift and transverse relaxation data for the tubercidin H-2 resonance gave inconsistent results for the chemical shift of the bound species and was inconsistent with the assumption of a single, bound conformation. These results were interpreted in terms of a 2:1 ratio of a *syn*, 3′-*exo*:*anti*, 3′-*endo* geometry for bound tubercidin. Ligand competition experiments using 9-deazainosine show that all of the tubercidin TRNOE effects are reversed by addition of the second nucleoside, suggesting that the TRNOE data for tubercidin arise due to interactions at the active sites of PNP rather than as a consequence of nonspecific binding to the enzyme.

Purine nucleoside phosphorylase[1] (PNP) (EC 2.4.2.1) catalyzes the reversible phosphorolytic cleavage of purine ribonucleosides and deoxyribonucleosides. Inhibition of this enzyme has been proposed to potentially provide a means for suppression of cellular immunity. Selective immunosuppression and elevated dGTP levels have been observed in patients lacking PNP (Giblett, 1975). PNP inhibition might also be useful for the treatment of hyperuricemia or to increase the duration of action of chemotherapeutic nucleoside analogs. Significant efforts have thus been undertaken to design and synthesize more effective inhibitors of PNP.

The PNP produced by *Escherichia coli* consists of six structurally identical subunits, each subunit having a molecular weight of 22.5 kDa and one active site (Jensen & Nygaard, 1975). This enzyme has been used extensively as a catalyst for the synthesis of nucleoside analogs (Krenitsky et al., 1981) and it can have a significant impact on antiviral drug bioavailability due to its role in nucleoside metabolism by intestinal flora (Avramis & Plunkett, 1982). Characteristics which enhance its synthetic value—stability and availability—favor its use in NMR studies of ligand-binding interactions. Although the enzyme has been crystallized and X-ray diffraction studies at 3.0 Å are in progress (Cook et al., 1987), detailed data on the conformation of substrates or inhibitory nucleosides bound at the active site are as yet unavailable. Nevertheless, some insight into the conformation of bound nucleosides has been deduced from the substrate and inhibitory data obtained from nucleosides which exhibit strong conformational preferences or are conformationally constrained (Doskocil & Holy, 1977). In particular, the carbocyclic analog of adenosine, aristeromycin, which was demonstrated to adopt a *syn* geometry in solution (Holy, 1976), is not a substrate for PNP and has negligible inhibitory activity. Similarly, the analog 8-bromoadenosine, which strongly favors a *syn* geometry in solution (Miles et al., 1970; Ikehara et al., 1972; Jordan & Niv, 1977a) is ineffective as an inhibitor of PNP activity (Doskicil & Holy, 1977). These results have been taken as evidence that bound nucleosides adopt a

* Address correspondence to this author at Laboratory of Molecular Biophysics, MD 17-05, National Institute of Environmental Health Sciences, Box 12233, Research Triangle Park, NC 27709.

[†] National Institute of Environmental Health Sciences.

[§] Current address: Cambridge NeuroScience, Cambridge, MA 02139.

[∥] Wellcome Research Laboratories.

[⊕] Abstract published in *Advance ACS Abstracts,* June 1, 1994.

[1] Abbreviations: CPMG, Carr–Purcell–Meiboom–Gill version of the T_2 experiment; 9-DI, 9-deazainosine; L/E, ligand/enzyme concentration ratio, with E corresponding to the concentration of enzyme subunits, i.e. equal to 6[E]; NMR, nuclear magnetic resonance; NOE, nuclear Overhauser effect; ROE, rotating-frame nuclear Overhauser enhancement; TRNOE, transferred nuclear Overhauser effect [this also refers to the name of the program described by London et al. (1991)]; TRROE, transferred rotating-frame nuclear Overhauser enhancement; PNP, purine nucleoside phosphorylase; Tris-d_{11}, perdeuterated tris(hydroxymethyl)-aminomethane.

geometry closer to *anti* about the glycosidic bond. In contrast, crystallographic data for C-nucleoside complexes with human erythrocytic PNP (Ealick et al., 1990) indicate a bound conformation with a glycosidic bond angle of $\chi = 110 \pm 10°$ (O4′–C1′–N9–C4) (S. Ealick, personal communication), closer to a *syn* or high *anti* geometry. However, there are substantial differences in structure and substrate preferences between bacterial and human forms of PNP (Cook et al., 1985).

Although the high molecular weight of PNP precludes direct ^{1}H NMR observations using currently available strategies, information about the conformation of complexed nucleoside inhibitors can be derived from transferred NOE studies (TRNOE), if the exchange between the complexed and uncomplexed states is sufficiently rapid. In such studies, the much greater cross-relaxation rates characterizing the bound species will dominate over the low cross-relaxation rates characterizing the free nucleoside. The conditions for applicability of these approximations have been considered by Clore and Gronenborn (1982, 1983):

$$p_B\sigma^B > p_F\sigma^F \quad (1)$$

$$k_{-1} \gg \sigma^B \quad (2)$$

where p_B and p_F are the fractions of bound and free nucleosides, and σ^B and σ^F the cross relaxation rates for the bound and free ligand, respectively. This approach has been widely applied to studies of nucleotides (Banerjee et al., 1985; Fry et al., 1987), nucleotide cofactors such as $NADP^+/NAD^+$ (e.g. Feeney et al., 1983; Clore & Gronenborn, 1983; Brito et al., 1991), and a wide variety of other small, reversibly complexed ligands [for reviews, see Craik and Higgins (1989), Gronenborn and Clore (1990), Neuhaus and Williamson (1989)].

Tubercidin (7-deazaadenosine) is a competitive inhibitor of *E. coli* PNP that does not undergo significant turnover and has an inhibition constant of $K_i = 18\ \mu M$ (J. Tuttle, unpublished results).

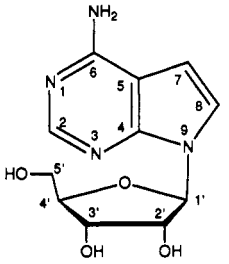

If the rate of binding to PNP is assumed to be diffusion controlled, the dissociation rate of the tubercidin–PNP complex is likely to be rapid enough to satisfy eq 2 above. We therefore concluded that the tubercidin–PNP complex represented a suitable system in which to carry out TRNOE measurements. One of the most significant limitations on the use of the TRNOE method arises as a result of the difficulty in distinguishing direct dipolar interactions from indirect NOE interactions which can be mediated by either ligand or enzyme protons. As discussed recently, the reliance on the observation of a lag in the development of the TRNOE as an indicator of significant indirect pathways is hazardous since such lags may be produced by other factors, such as slow exchange on the chemical shift time scale (Kohda et al., 1987; London et al., 1992), or be absent in the case of intermediate rates of chemical exchange (London et al., 1992). Additionally, for large macromolecules such lags may be of very short duration, and hence not readily observable. As a result of the dependence of the TRNOE on the exchange rate, measurements of the ligand-exchange rate were also undertaken.

In order to further sort out the contributions of direct and indirect relaxation pathways, we have also carried out transferred ROE (TRROE) measurements on this system. Comparisons of NOE and ROE buildup curves in macromolecules have previously been reported to be useful for separation of direct and indirect dipolar relaxation pathways (Fejzo et al., 1989; Bauer et al., 1990). We have investigated the application of TRROE for analysis of spin diffusion contributions to the TRNOE buildup curve. The combination of this approach with back-calculation of TRNOE and TRROE curves using relaxation matrix calculations that employ experimentally determined exchange rates has further supported the proposal of two binding modes for tubercidin.

MATERIALS AND METHODS

Materials. Purine nucleoside phosphorylase was purified from *E. coli* using an ether-linked formycin B/Sepharose 6B resin with unusual properties (Hall & Krenitsky, 1990). The enzyme was dialyzed six times against D_2O, using 50 mL each time. The specific activity was determined using the inosine/xanthine oxidase method (Tuttle & Krenitsky, 1984) to be 60 units/mg, corresponding to a concentration of 0.7 mM in active enzyme subunits (all enzyme concentrations discussed hereafter are reported per subunit).

Tubercidin was obtained from Sigma, and 9-deazainosine was prepared by the method of Lim et al. (1983). [2′-^{2}H]-Tubercidin (98% ^{2}H) was prepared from unlabeled tubercidin (Perlman, 1993). Tris-d_{11} was purchased from MSD Isotopes.

Sample Preparation. Stock solutions of the ligand in D_2O were adjusted to pH 7.4, lyophilized, and redissolved in D_2O, and the ligand concentration was determined by UV spectrophotometry ($\epsilon = 1.2 \times 10^4\ cm^{-1}\ M^{-1}$ at 270 nm, neutral pH) (Pike et al., 1964). Solutions of ligand and enzyme/ligand mixtures were prepared in 20 mM Tris-d_{11}, 0.1 mM EDTA, 2.0 mM *t*-BuOH, and 0.1 mM NaN_3 in D_2O at pH 7.4 (pH measurements were obtained using a glass electrode standardized in H_2O buffers and were uncorrected for isotope effects). Enzyme activity of both the stock and NMR solutions was monitored periodically as described above to assure stability.

NMR Spectroscopy. ^{1}H NMR spectra were obtained at 500 MHz on a GN-500 (General Electric) with quadrature detection. Chemical shifts are reported relative to TMS using *t*-BuOH as an internal standard (1.25 ppm). Samples were run in either 5- or 10-mm tubes, the latter being preferred due to the use of low concentrations required by the poor solubility of tubercidin. TRNOE spectra were obtained using a 1-D selective inversion recovery pulse senquence (Anderson et al., 1985):

$$\text{RD–180°(on)–}\tau_m\text{–90°–Acq(+)–RD–180°(off)–}\tau_m\text{–90°–Acq(–)} \quad (3)$$

with low power saturation of the residual HDO signal in D_2O solutions during RD and τ_m. Alternate FID's acquired with selective inversion in the protein envelope at 3 ppm (off) were subtracted in memory from those obtained with inversion at a ligand resonance (on). The relaxation delay (RD) was adjusted for each setting of τ_m so that the recycle time (RD + τ_m + Acq) remained at 2–3 times the value of the longest T_1 of interest, so that relaxation would occur to the same extent for each mixing time (Eaton & Anderson, 1987).

Transferred ROE spectra were also acquired as 1-D difference spectra, using the CAMELSPIN experiment (Bothner-By et al., 1984) as described by the pulse sequence below:

$$\text{RD–180°(on)–90°–}\tau_m\text{(SL)–Acq(+)–RD–}\tau\text{–90°–}\tau_m\text{(SL)–Acq(–)} \quad (4)$$

The delay τ was set to the length of a 180° pulse and HDO presaturation was conducted during RD. A spin-locking field (SL) of 2 kHz was centered at the HDO resonance and was achieved using a train of 5-ms pulses. Equilibration was achieved with the use of at least eight dummy scans prior to accumulation. A spectral width of 6 kHz was employed with acquisition of 4K data points.

Spin–lattice relaxation times were measured as selective T_1's using the pulse sequence RD-sel 180°–t_1–90°–Acq, where RD is at least 5 times T_1. T_2 values for studies of variation of L/E were measured using a Hahn echo experiment, or were based on line widths ($\Delta\nu$) of uncoupled resonances measured at half-height ($1/T_2 = \pi\Delta\nu$)) (after correcting for line broadening due to field inhomogeneity based on the signal for t-BuOH). Methods used to perform CPMG and $T_{1\rho}$ experiments are described elsewhere (Davis et al., 1994).

Enhancements, $\Delta I(\tau_m)$ were normalized relative to the average of the intensity normalized, selective T_1 curves for the pair of interacting spins I and S (Macura et al., 1986):

$$f_I\{S\}(\tau_m) = \frac{\Delta I(\tau_m)}{\frac{1}{2}[I(\tau_m) + S(\tau_m)]} \quad (5)$$

The selective T_1 curves $I(\tau_m)$ and $S(\tau_m)$ are normalized so that the denominator decays from 1.0 to 0 as $\tau_m \rightarrow \infty$. This procedure is analogous to dividing the cross peaks in a 2D NOESY experiment by an average of the corresponding diagonal elements. The application of eq 5 has the effect of extending the linear region of the NOE or ROE buildup curve so that the determination of the initial slope is greatly facilitated. For the remainder of the paper, we further abbreviate $f_I\{S\}$ as $I\{S\}$, and so forth.

In addition, an offset and NOE correction was performed on the observed ROE data using the relationship

$$\sigma^r_{IS} = \frac{\sigma^r_{obs} - \cos\theta_I \cos\theta_S \sigma^n_{IS}}{\sin\theta_I \sin\theta_S} \quad (6)$$

where S = inverted, I = observed, σ^r_{IS} = corrected ROE, σ^r_{obs} = observed ROE, and σ^n_{IS} = observed NOE, and $\theta = \tan^{-1}(\gamma\beta_1/\Delta\omega_i)$, with $\Delta\omega_i$ = offset of S or I from transmitter (radians) (Davis, 1987). The ROE buildup curves $\sigma^r_{IS}(\tau_m)$ can be normalized analogously to the NOE buildup curves, with offset effects also taken into account (Brown & Farmer, 1989).

Cross-relaxation data have been presented using signs which are consistent with the relationship of $\Delta I(\tau_m)$ in the difference spectrum to the negatively phased inverted peak, $S(\tau_m)$. Thus, peaks with the same sign as the inverted peak yield a negative cross-relaxation rate and negative buildup curves, although the latter are displayed as positive here for ease of viewing. The sign convention used here is opposite of that used in our recent theoretical treatment (London et al., 1992), which was intended to be consistent with that used for 2-D NOESY spectra, wherein the diagonal peaks are normally positively phased.

Studies of Exchange Kinetics. Variations in the NMR parameters of ligands in the presence of exchange with macromolecule binding sites have been treated within the context of a two-state model corresponding to the uncomplexed and enzyme complexed states (Sykes & Scott, 1972; Swift & Connick, 1962).

$$E + I \underset{k_{-1}}{\overset{k_1}{\rightleftharpoons}} EI \quad (7)$$

Imposing the additional constraint that the fraction of inhibitor which is bound to the enzyme, p_B, is small, the observed chemical shift, δ_{obs}, and transverse relaxation time, T_2^{obs}, can be expressed in terms of apparent values for the bound state according to

$$\delta_{obs} = p_F\delta_F + p_B\Delta\delta^{app} \quad (8)$$

where

$$\Delta\delta^{app} = \frac{(\delta_B - \delta_F)}{\left(1 + \frac{\tau_B}{T_{2B}}\right)^2 + (\tau_B\Delta\omega)^2} \quad (9)$$

and

$$\frac{1}{T_2^{obs}} = \frac{p_F}{T_{2F}} + \frac{p_B}{T_{2B}^{app}} \quad (10)$$

where

$$\frac{1}{T_{2B}^{app}} = \frac{1}{T_{2B}}\left[\frac{\left(1 + \frac{\tau_B}{T_{2B}}\right) + T_{2B}\tau_B\Delta\omega^2}{\left(1 + \frac{\tau_B}{T_{2B}}\right)^2 + (\tau_B\Delta\omega)^2}\right] \quad (11)$$

where T_{2F} and T_{2B} are the transverse relaxation rates of the uncomplexed ligand and bound ligand, respectively, $\tau_B = 1/k_{-1}$ is the lifetime of the bound inhibitor, and $\Delta\omega = 2\pi(\delta_B - \delta_F)$ is the chemical shift difference of a particular ligand resonance between uncomplexed and complexed states. Values of $\Delta\delta^{app}$ and $1/T_{2B}^{app}$ can be obtained by varying p_B (eqs 8 and 10, respectively), while estimates of T_{2B} are provided from CPMG and $T_{1\rho}$ measurements (below). For typical macromolecular T_{2B} and $\Delta\omega$ values, significant differences can exist between the intrinsic $\delta_B - \delta_F$ and $\Delta\delta^{app}$ (eq 9) and between $1/T_{2B}$ and $1/T_{2B}^{app}$ (eq 11). Therefore, from the dependence of $\Delta\delta^{app}$ or $1/T_{2B}^{app}$ on temperature (and thus k_{-1}), one can calculate values of τ_B (i.e. $1/k_{-1}$) and $\Delta\omega$ using eq 9 or 11.

A more direct method for determination of ligand-exchange rates used by Gerig and co-workers (Gerig & Stock, 1975) involves Carr–Purcell–Meiboom–Gill (CPMG) measurements of the transverse relaxation rate as a function of the pulsing rate, $1/t_{cp}$, where t_{cp} is the interval between successive 180° pulses. Solutions of this problem for a sufficiently general case have been obtained by Carver and Richards (1972) and corrected by Stock (1974) and by Jen (1978). The measurement of $T_{1\rho}$ as a function of the strength of the spin-lock field (ω_{SL}) has also been employed previously in studies of ligand-exchange behavior (Deverell et al., 1970; Laszlo, 1979, and references therein), but we are not aware of any application to a biological system. The dispersion curve obtained in this case can be shown based on the results of Deverell et al. (1970) and Wennerstrom (1972) to be described by

$$\frac{1}{T_{1\rho}} = \frac{p_F}{T_{1\rho}^F} + \frac{p_B}{T_{1\rho}^B} + \frac{p_F p_B \Delta\omega^2/k}{1 + (\omega_{SL}k)^2} \quad (12)$$

where the off-rate $k_{-1} = p_F k = 1/\tau_B$. A detailed discussion

of the derivation of the expressions describing the CPMG and $T_{1\rho}$ experiments, and the application of these experiments to obtaining values of k_{-1} for the tubercidin–PNP system has been described elsewhere (Davis et al., 1994). In both experiments, a sigmoidal curve is generated, with an inflection point corresponding to a pulse rate which is similar to the ligand-exchange rate. The results from Hahn echo experiments are utilized to fit data at both low pulse rates or low spin-lock fields, due to the lower accuracy of the CPMG and $T_{1\rho}$ methods at these limits. A L/E ratio of 10 instead of 40 was utilized for rate determinations at 20 °C in order to increase the dispersion between the limits of $1/T_2$ or $1/T_{1\rho}$. Data were fit to the appropriate expressions by varying T_{2B}, $\Delta\omega$, and k_{-1}.

Ligand Competition Experiments. The effect of the presence of a second inhibitor, S, with enzyme dissociation constant, K_S, on the fraction of ligand I which is complexed to the enzyme, p_B, can be expressed as

$$p_B = \{E_o(1-R) - S_o - RI_o + [\{S_o + RI_o - E_o(1-R)\}^2 + 4RI_oE_o(1-R)]^{1/2}\}/2I_o(1-R) \quad (13)$$

where p_B is the fraction of the observed ligand complexed with the enzyme, $R = K_S/K_I$, the ratio of the dissociation constants of the two inhibitors, and I_o and S_o are the initial (total) concentrations of the observed ligand ([2′-^{2}H]tubercidin) and the second ligand (9-deazainosine), respectively. Equation 13 above is derived subject to the assumption that all of the enzyme is complexed to either of the inhibitors I or S.

Detection of Spin Diffusion Using the Transferred ROE. As demonstrated by our recent theoretical simulations, spin diffusion pathways can also contribute significantly to the observed TRNOEs (London et al., 1992). It has been pointed out by Markley and co-workers (Fejzo et al., 1989, 1990) and by Bauer et al. (1990) that a comparison of NOE and rotating-frame Overhauser enhancement (ROE) interactions between spins in a macromolecule can provide additional insight into the possible significance and analysis of spin diffusion pathways. For a ligand/macromolecule system with size and kinetic properties which satisfy eqs 1 and 2, the buildup curves for the bound ligand in a TRNOE and TRROE experiment, with an indirect pathway between i and j mediated by spin k, can be described by eqs 14 and 15, respectively:

$$a_1^{nB} = -\left\{\tau_m p_B \frac{k'\tau_c^B}{(r^B_{ij})^6} + \frac{1}{2}\tau_m^2 p_B^2 \sum_{k\neq i,j}\left[\frac{k'\tau_c^B}{(r^B_{ik})^6}\right]\left[\frac{k'\tau_c^B}{(r^B_{kj})^6}\right]\right\} \quad (14)$$

$$a_1^{rB} = 2\left\{\tau_m p_B \frac{k'\tau_c^B}{(r^B_{ij})^6} - \tau_m^2 p_B^2 \sum_{k\neq i,j}\left[\frac{k'\tau_c^B}{(r^B_{ik})^6}\right]\left[\frac{k'\tau_c^B}{(r^B_{kj})^6}\right]\right\} \quad (15)$$

where $k' = 0.1(\mu_o/4\pi)^2(h/2\pi)^2\gamma^4$. Note that a_1^r and a_1^n are assumed to already have been normalized relative to the diagonal at τ_m using eq 5. These equations are identical to those for the nonexchanging system (Fejzo et al., 1989), except for the presence of p_B in the linear term and p_B^2 in the quadratic term. Thus, an indirect dipolar relaxation pathway will still result in an increase in the observed NOE, but it will lead to a much more rapid decrease in the magnitude of the ROE, due to the sign change and the 4-fold higher coefficient of the quadratic term in eq 15. Of course, higher order terms involving multiple polarization transfers may also be significant in complex spin systems.

Therefore, spin diffusion involving a protein or ligand (depending on geometry) spin under conditions of fast exchange should be revealed by a direct comparison of "bound" NOE and ROE curves after subtraction of $p_F\sigma^F_{ij}\tau_m$, where the latter is determined from experiments performed in the absence of enzyme. A direct comparison can then be made by multiplying the ROE data by $-1/2$ to correct for the differences in the coefficients of the linear terms of eqs 14 and 15. Any differences between the NOE and ROE buildup curves can then be ascribed to an indirect pathway via spin k, wherein sufficiently small r_{ik} and r_{kj} distances relative to r_{ij} exist to make the second, quadratic terms in the above equations cause a deviation from linearity. Alternatively, a nonlinear bound buildup curve can be fit to a quadratic equation and σ_{ij} obtained from the linear coefficient. However, if more than one spin is responsible for a difference between the NOE and ROE curves, as is likely for spin diffusion involving protein spins, or if exchange is not sufficiently rapid, then simulation of the buildup curve using relaxation matrix calculations (below) is more suitable.

Molecular Modeling and Relaxation Matrix Calculations. The crystal structure of tubercidin (Abola & Sundaralingam, 1973) provided the starting geometry for molecular mechanics calculations using the CHARMm force field with the QUANTA interface (Polygen) on an IRIS 4D/70G workstation (Silicon Graphics). Simulations of TRNOE buildup curves were performed using the program TRNOE (London et al., 1992) written in Mathematica for a Macintosh. A combination of relaxation and kinetic matrices provides an expanded $2n \times 2n$ relaxation matrix as described previously. Calculations for the transferred ROE (TRROE) analogous to those described previously for the TRNOE can be carried out by using the appropriate spectral density terms (Bothner-By et al., 1984):

$$\rho_{ij} = \frac{h^2\gamma_i^2\gamma_j^2}{(2\pi)^2 r_{ij}^6}[2.5J_0(\omega) + 4.5J_1(\omega) + 3J_2(\omega)] \quad (16)$$

$$\sigma_{ij} = \frac{h^2\gamma_i^2\gamma_j^2}{(2\pi)^2 r_{ij}^6}[3J_1(\omega) + 2J_0(\omega)] \quad (17)$$

The elements of the relaxation matrices for the enzyme-complexed and uncomplexed ligand, $\mathbf{R_B}$ and $\mathbf{R_F}$, are then given by

$$R_{ii} = \sum_j \rho_{ij} + \rho^* \qquad R_{ij} = \sigma_{ij} \quad (18)$$

For the calculations presented here, isotropic motion has been assumed, so that a single correlation time is used for all of the protons in each of the ligand states. For TRNOE calculations, a value of $\rho^* = 1\ s^{-1}$ is generally assumed, corresponding to the leakage of the net polarization via relaxation sinks in the protein (London et al., 1992). Additional contributions to ρ^* from exchange processes or relaxation interactions with protein protons not explicitly included in the matrix can in principal significantly reduce the observed ROE effects. For either the TRNOE or TRROE calculation, solution of the differential equation

$$\frac{dA}{dt} = -(\mathbf{R} + \mathbf{K})\mathbf{A} \quad (19)$$

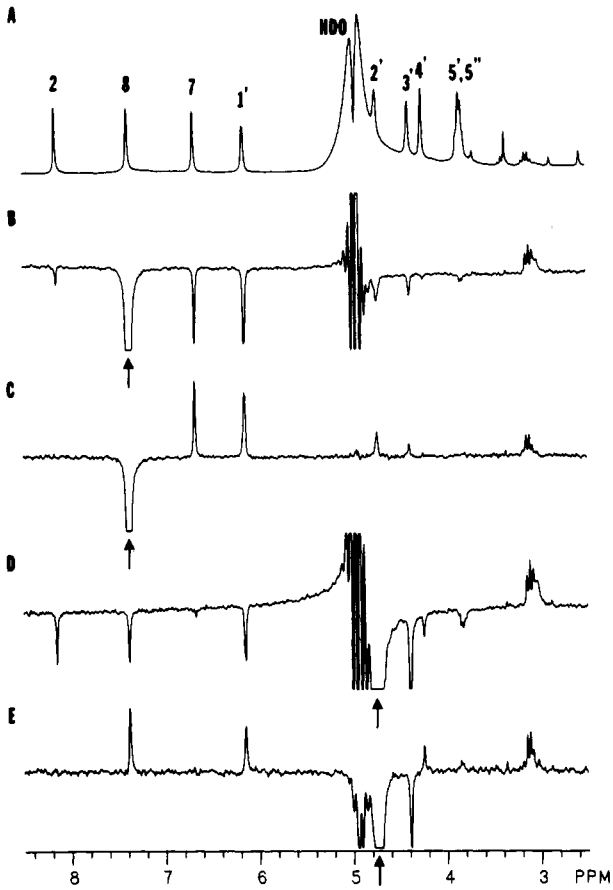

FIGURE 1: 500-MHz ^{1}H NMR spectra of a solution of tubercidin and PNP at 10 °C (L/E = 40, [L] = 1.5 mM): (A) One-pulse spectrum; difference spectra for selective inversion at H-8 for (B) TRNOE and (C) TRROE and for selective inversion at H-2′ for (D) TRNOE and (E) TRROE. Mixing time (τ_m) of 200 ms used for all difference spectra. Number of scans: (A) 40, (B) 2000, (C–E) 3200.

where **R** and **K** correspond to the appropriate expanded relaxation and kinetic matrices, yields the matrix of cross peak intensities, **A**. A collapsed "**C**" matrix, which corresponds to the crosspeak intensities for a system in fast exchange on the chemical shift scale, is generated, and the C_{ij} elements of the intensity matrix are then normalized relative to the average of C_{ii} and C_{jj}, in analogy with the scaling procedure for the experimental data employing eq 5.

RESULTS

Determination of TRNOE Buildup Curves for Tubercidin–PNP. TRNOE experiments were performed on a 40:1 ratio of tubercidin–PNP at 20 °C using selective-inversion recovery difference spectra to minimize spin diffusion and improve selectivity (Anderson et al., 1985). Strong, negative NOE's were observed for inversion of H-8 at both H-1′ and H-3′ (Figure 1B) and for inversion of H-2′ at both H-8 and H-2 (Figure 1D). Inversion at H-2′ was conducted at 10 °C, in order to reduce the overlap of the H-2′ resonance with the residual HDO resonance. Spectra were then obtained at a variety of mixing times (τ_m) in order to examine the NOE buildup curves for evidence of spin diffusion. As a consequence of the method employed for normalization of the enhancements (eq 5), NOE buildup curves which are dominated by direct interactions *should* exhibit linear buildup curves out to mixing times of at least 0.5 s. Linear buildup curves were obtained for the interactions 8{1′}, 8{3′}, and 8{7} (Figure 2A) ($I\{S\}$, where I = observed and S = inverted). Even at very early mixing times (less than 50 ms), it was still not possible to detect any lag period indicative of an indirect effect. Linear

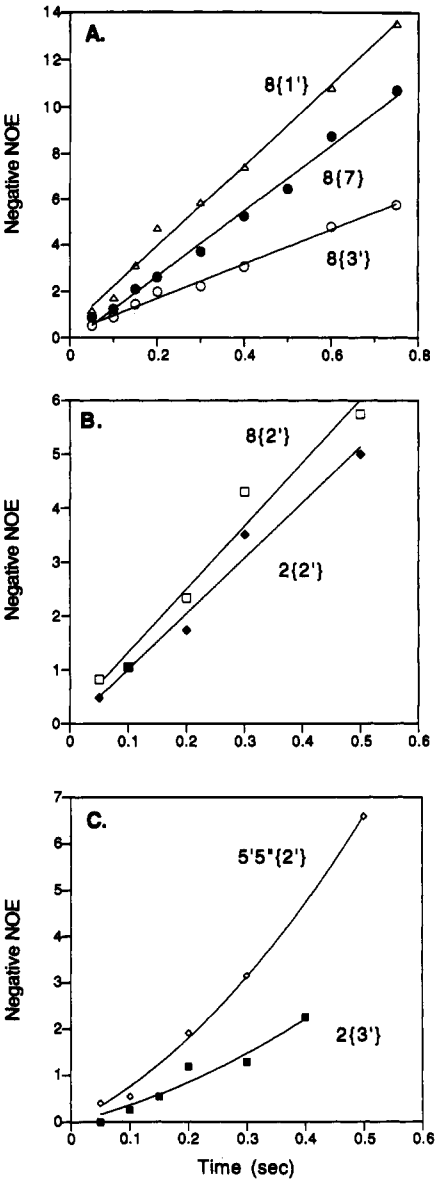

FIGURE 2: Normalized TRNOE buildup curves (eq 5) for tubercidin–PNP (L/E = 40, [L] = 1.5 mM) obtained at 20 °C (A, 2{3′} in C) or 10 °C (B, 5′5″{2′} in C) ($I\{S\}$ where S = inverted spin): △, 8{1′}; ●, 8{7}; ○, 8{3′}; □ 8{2′}; ◆, 2{2′}; ◇, 5′5″{2′}; ■, 2{3′}. Lines are for linear (A, B) or quadratic (C) fits to data.

buildups were also obtained for 2{2′} and 8{2′} (Figure 2B). The curve for 5′,5″{2′} exhibited a slight nonlinearity and 2{3′} a more destinct lag period (Figure 2C).

If the constraints given by eqs 1 and 2 are satisfied, the observed cross-relaxation rates will satisfy the relation (Clore & Gronenborn, 1983):

$$\sigma^{obs} = p_B\sigma^B + p_F\sigma^F \approx p_B\sigma^B \qquad (20)$$

For those interactions which appeared to be dominated by direct dipolar interactions as evidenced by a linear NOE buildup curve, cross-relaxation rates, σ_{ij}, were obtained from the slopes. Internuclear distances, r_{ij}, were calculated using eq 21 (Clore & Gronenborn, 1983) and the fixed distance r_{78} = 2.71 Å from the crystal structure of tubercidin (Abola & Sundaralingam, 1973) as a reference distance:

$$r_{ij}/r_{78} = (\sigma_{78}/\sigma_{ij})^{1/6} \qquad (21)$$

None of resulting distances $r_{81'}$, $r_{82'}$, and $r_{83'}$ determined for the bound ligand (Table 1) exceed 3.2 Å; the data are thus

Table 1: Observed Transferred NOE Cross-Relaxation Rates (σ^a) for Apparent Direct Effects and Resulting Internuclear Distances (r)[b]

ligand protons		40:1 tubercidin–PNP										
		20 °C		10 °C		40:1 [2′-²H]tubercidin–PNP (20 °C)				tubercidin (20 °C)		crystal structure:[c]
I	S	σ	r	σ	r	σ	r	$\sigma^{B\,d}$	r	σ^F	r	r
8	7	−0.142	2.71[c]	−0.208	2.71[c]	−0.120	2.71[c]	−6.38	2.71[c]	0.0481	2.71[c]	2.71
8	1′	−0.175	2.62	−0.293	2.56	−0.214	2.46	−8.78	2.57	0.0298	2.94	3.73
8	2′			−0.117	2.98					0.0439	2.75	2.15
8	3′	−0.0743	3.02	−0.078	3.19	−0.075	2.93	−5.01	2.82	0.00718	3.72	4.45
1′	2′			−0.118	2.98					0.0154	3.28	3.01
2	2′			−0.103	3.06					0.0460	2.73	6.76

[a] Cross-relaxation rate (s^{-1}) between I (observed spin) and S (inverted spin) from initial slope of NOE buildup curve in s^{-1}, normalized using eq 5. Maximum error in σ = 10%. [b] Distances r_{IS} calculated from σ_{IS} and σ_{78} using eq 21. Maximum error in calculated distances is ±0.15 Å. [c] Reference distance from crystal structure (Abola & Sundaralingam, 1973). [d] Cross-relaxation rate for bound ligand calculated using Figure 3A and eq 20.

inconsistent with any single conformation about the glycosidic bond for PNP-complexed tubercidin. Similarly, the short distances for both $r_{22'}$ and $r_{82'}$ are also incompatible with a single conformation. However, $\sigma_{1'2'}$ yields a value of 2.98 Å for r_{12} (Table 1) that is consistent with the crystal data (3.01 Å).

The failure of the TRNOE data to provide distance constraints which are consistent with a single, bound conformation of the molecule has several potential explanations: (1) Indirect relaxation pathways mediated through either the ligand protons or protons on the enzyme that are efficient enough not to be associated with an observable nonlinearity in the buildup curves. (2) Significant contributions to the observed TRNOE from the free species invalidate the distance information obtained, which is based on the assumption (eq 1) that the NOE's in the free species can be neglected. (3) Ligand exchange is insufficiently rapid compared with the relevant cross-relaxation rates of the bound species and therefore alters the observed NOE buildup curves. This effect leads to systematic errors since NOE buildup rates between directly interacting spins are underestimated, while those mediated by indirect dipolar coupling pathways are overestimated (London et al., 1992). (4) There may be multiple modes of binding. A series of studies was designed to determine the possible significance of each of these effects.

Effect of Selective Deuteration of the Ligand on TRNOE Results. On the basis of an initial analysis of the likely conformations of tubercidin, H-2′ appeared to be the only ligand proton that could play an important role in the mediation of indirect dipolar coupling pathways between H-8 and H-1′ or H-3′. Therefore, TRNOE experiments were conducted using tubercidin deuterated at H-2′ (Perlman, 1993) in the presence of PNP. However, the cross-relaxation rates obtained from the buildup curves were found to be sufficiently close to those for the unlabeled compound to cause only minor alterations in the distances (Table 1). Consequently, ligand-mediated spin diffusion pathways appear to be of minimal significance for the NOE interactions between H-8 and the sugar protons which define the glycosidic angle. The [2′-²H]tubercidin used in the above studies was also found to be useful for studies of the tubercidin-exchange rate, which are ideally performed on nuclei (such as H-1′) which are not scalar-coupled to other spins.

Studies of Variation in L/E Ratio. The enzyme concentration (in subunits) was varied from no enzyme to 0.3 mM (L/E = 5:1) with the concentration of [2′-²H]tubercidin held constant at 1.5 mM. At each ratio the values of the chemical shifts, of $1/T_2$, and of σ from TRNOE buildup curves were determined. The results are shown in Figure 3. The linearity of these plots, as well as those obtained for $1/T_1$ (selective; data not shown), indicates that enzyme aggregation and nonspecific binding are not significant factors. The linear

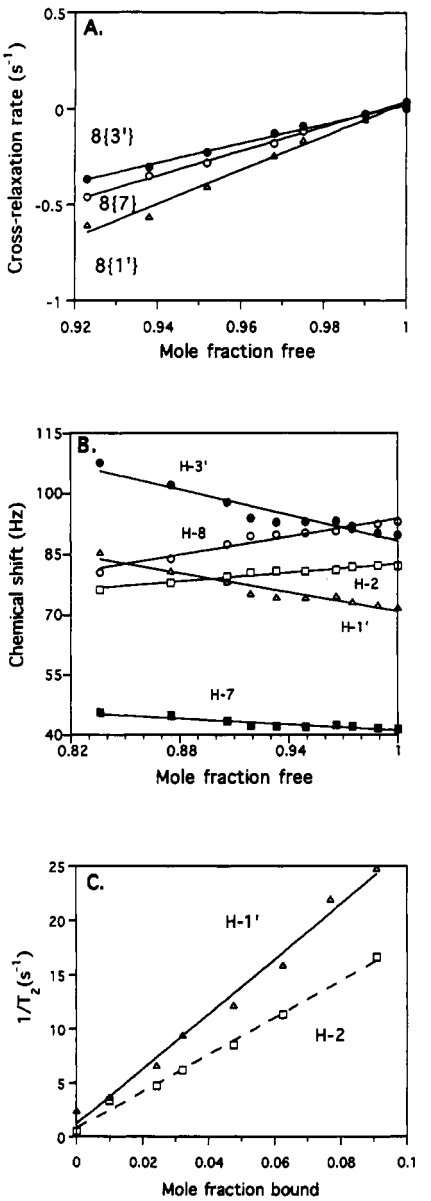

FIGURE 3: Dependence on mole fraction free (p_F) or bound (p_B) of 1.5 mM [2′-²H]tubercidin in presence of varying concentrations of PNP at 20 °C for (A) cross-relaxation rate (●, 8{3′}; ○, 8{7}; △, 8{1′}), (B) chemical shift (○, H-8; ●, H-3′; □, H-2; △, H-1′; ■, H-7) relative to arbitrary reference, and (C) transverse relaxation rate (△, H-1′; □, H-2).

variation of the cross-relaxation rates (σ^{obs}) with the mole fraction of free ligand (p_F) (Figure 3A) over a range that includes the 40:1 ratio used in this study to as low as 12:1 is consistent with eq 20.

No significant nonlinearity in any of the buildup curves used to determine σ^{obs} was exhibited at any ratio, including

100:1, where lower cross-relaxation rates would be expected to facilitate observation of a lag period. The cross-relaxation rate for the bound species, σ^B, for each interaction was determined by extrapolation to $p_F = 0$ (Table 1). However, internuclear distances calculated from σ^B differed by no more than 0.1 Å from those calculated using σ^{obs} at 40:1, which indicates that the contribution of the positive NOE's from the free ligand (σ^F) does not have a significant effect on the distances obtained for measurement at this ratio.

Estimation of the Ligand-Exchange Rate. A. Analysis Using Swift and Connick Relationships. Measurements of the chemical shifts for [2′-^{2}H]tubercidin relative to the methyl resonance of *tert*-butyl alcohol at 20 °C as a function of p_B in the range $0 < p_B < 0.2$ yielded straight lines (Figure 3B) from which apparent chemical shift differences, $\Delta\delta^{app}$, were determined from the slopes for the various resonances (eq 8). As noted in the previous section, the measured shifts will only correspond to the actual shifts for exchange rates sufficiently rapid such that k_{-1} ($=1/\tau_B$) $\gg 1/T_{2B}$, $\Delta\omega$, so that the denominator of eq 9 approaches 1. In fact, the $\Delta\delta^{app}$ were found to decrease with decreasing temperature. This behavior is consistent with predictions from eq 9 if the primary temperature dependence arises from the temperature dependence of k_{-1}. Thus, at higher temperatures, shorter k_{-1} values will make $\Delta\delta^{app}$ approach the actual $\Delta\delta$ value. As a result of the dependence of $\Delta\delta^{app}$ on temperature, these data can be used to derive a rough estimate for k_{-1}, as described in detail in the supplementary material section. Optimal k_{-1} values of 800, 2000, and 5000 s^{-1} at 10, 20, and 30 °C were obtained in this way, with $\Delta\delta$ values of 40 and 90 Hz for H-2 and H-1′, respectively. Values for other protons are included as supplementary material.

Following a similar approach, the observed $1/T_2$ values for the two nonscalar coupled protons H-2 and H-1′ of [2′-^{2}H]-tubercidin were determined using either Hahn spin-echo or line width measurements. As in the case of the chemical shift measurements, $1/T_{2B}^{app}$ values taken from the slopes of the $1/T_2^{obs}$ vs p_B curves, were found to exhibit a significant temperature dependence, with values of 255, 234, and 160 s^{-1} obtained at 10, 20, and 30 °C, respectively (data for 20 °C shown in Figure 3C). Dissociation rate constants $k_{-1} = 1/\tau_B$ can be determined from eq 11 if the values of $1/T_{2B}$ are known. Estimating the value of T_{2B} from $T_{1\rho}$ data *(vide infra)*, most of the temperature dependence of the $1/T_{2B}^{app}$ data is seen to arise from the temperature dependence of τ_B. Fitting the data as described in the supplementary material section yielded k_{-1} values of 1640, 1780, and 3720 s^{-1} at 10, 20, and 30 °C derived from the $1/T_2$ data for the H-1′ resonance. Data for H-2 were also found to be temperature dependent, with values of 265, 187, and 138 s^{-1} at 10, 20, and 30 °C, respectively. However, fundamental problems were encountered in the attempt to fit the H-2 data using this approach. In particular, it was not possible to fit the 10 and 20 °C $1/T_{2B}^{app}$ data using the value of $\Delta\delta = 40$ Hz obtained from direct chemical shift measurements of H-2 described above. This was true even if the T_{2B} value was allowed to vary by a factor of 3. This problem is described in more detail in the supplementary material.

The failure of the approach outlined above to yield a self-consistent set of parameters for the H-2 resonance is significant and indicates that the basic model described by eq 7 is not completely adequate to describe this system. Although several potentially complex alternative explanations are feasible, the most likely interpretation for the inconsistency noted above is the existence of significant binding heterogeneity; i.e. the hypothesis that tubercidin binds to PNP in at least two significantly different conformations. For the case of two bound conformations, the observed shift for H-2 can be very small if the two bound conformations shift the resonance in opposite directions: $\Delta\delta = \Delta\delta_A + \Delta\delta_B$, with $\Delta\delta_A$ and $\Delta\delta_B$ having opposite signs. However, the relaxation parameters will experience larger exchange contributions proportional to $(\Delta\delta_A)^2$ and $(\Delta\delta_B)^2$. This model is discussed further in subsequent sections.

B. Determination of Dissociation Rate Constant Based on T_2(CPMG) and $T_{1\rho}$ Measurements. The assumptions required to calculate exchange rates from the temperature dependence of $\Delta\delta^{app}$ or $1/T_{2B}^{app}$, most importantly the need to know or independently determine T_{2B}, limit the utility of such approaches. Therefore, measurements of k_{-1} were also performed using CPMG measurements of T_2 as a function of the pulsing rate, $1/t_{cp}$ (Gerig & Stock, 1975; Stock, 1974). An alternative and closely analogous approach involves the measurement of $T_{1\rho}$ as a function of the strength of the spin-lock field (Deverell et al., 1970; Laszlo et al., 1979, and references therein). The latter approach is somewhat simpler in practice, and can be analyzed using eq 12, but is limited in principle to exchange rates which fall into the fast exchange limit. A more complete discussion of these measurements is given by Davis et al. (1994), and results for the tubercidin–PNP system are summarized in the supplementary material. In either case, multiparameter fits were used to determine values for k_{-1}, $\Delta\delta$, and T_{2B}. The off-rates measured by either method give similar results, i.e. k_{-1} of about 2100 s^{-1} at 20 °C and 1400 s^{-1} at 10 °C, and values of T_{2B} = 9–10 ms. For H-1′, the data were fit to a dispersion curve using a value of $\Delta\delta$ of 110 Hz, in reasonable agreement with the value of 90 Hz derived from studies in which the fraction of tubercidin bound to the enzyme was varied. However, this was not the case for H-2, as the chemical shift parameter needed to fit either the CPMG or $T_{1\rho}$ data was 80 Hz, double the value of 40 Hz obtained from concentration-dependent studies.

This discrepancy is analogous to the problems encountered in fitting data for H-2 using eq 11. As noted above, the simplest resolution of the inconsistent results for H-2 is the hypothesis of two bound states, B1 and B2, each characterized by shifts relative to the free species, $\Delta\omega_{B1}$ and $\Delta\omega_{B2}$, of opposite sign. Presumably, the cancellation of $\Delta\omega_{B1}$ and $\Delta\omega_{B2}$ is greater in the case of H-2 than for H-1′. Furthermore, the relaxation parameters will experience larger exchange contributions proportional to $(\Delta\omega_{B1})^2$ and $(\Delta\omega_{B2})^2$ (as in eqs 9, 11, and 12). This appears to be the only satisfactory explanation of the observed relaxation data. The existence of two bound states with very different dissociation rate constants might be expected to result in more complex biphasic $1/T_2$ vs $1/t_{cp}$ curves, which were not observed in these studies (supplementary material). Thus, it is concluded that the dissociation rate constants for the ligand in the B1 and B2 states probably differ by less than 1 order of magnitude. Very high dissociation rate constants will obviously be missed using the above approaches, but would also be likely to characterize nonspecific binding, which was investigated as described below.

Ligand Competition Effects. The linearity of the plots in Figure 3 and their extrapolation at $p_F = 1$ to values close to those measured in the absence of enzyme suggests that nonspecific binding is not a significant factor in the results. However, in general the precision of the extrapolated values is poor and provides only a rough approximation of the degree of nonspecific binding. In order to further investigate nonspecific binding for [2′-^{2}H]tubercidin, TRNOE and T_1 measurements on deuterated tubercidin were conducted in the presence of a 10-fold excess of the inhibitor 9-deazainosine

Table 2: Relaxation Data for [2′-²H]Tubercidin in the Presence of 9-DI and PNP[a]

	T_1 (s)			σ (s^{-1})	
proton	obsd	calcd[b]	$I\{S\}$	obsd	calcd[c]
8	1.043	1.173	7{8}	−0.0335	−0.0403
7	1.65	2.11	1′{8}	−0.0724	−0.0743
1′	1.73	1.85	3′{8}	−0.00848	−0.0399

[a] Concentrations of 9-DI, [2′-²H]tubercidin, and PNP employed were 15.6, 1.5, and 0.075 mM, respectively, to yield a 208:20:1 ratio. [b] Calculated for $p_B = 0.0105$ using experimental dependence of T_1 on p_B (data not shown). [c] Calculated using $p_B = 0.0105$ from the curves in Figure 3A.

(9-DI; K_i = 50 μM). Using eq 13, one finds that if the equilibrium dissociation constants for the two ligands are assumed to be equal to the inhibition constants, $R = K_S/K_I = 2.78$, the fraction of tubercidin complexed to the enzyme will be reduced from $p_B \sim E_o/I_o = 0.05$ to $p_B = -0.0105$. Thus, relaxation parameters determined for $p_B = 0.05$ in the presence of the competing ligand should be equivalent to those determined at $p_B = 0.0105$ in the absence of the competing ligand. In general, the cross-relaxation rates and T_1 values measured for [2′-²H]tubercidin in the presence of 9-deazainosine were found to be consistent with this expectation (Table 2). The only significant percentage error corresponds to the case of 8{3′} for which the actual cross-relaxation values are very small. Therefore, the data are consistent with the conclusion that the two nucleoside inhibitors compete for a single class of binding sites to a degree which is quantitatively related to their inhibitory potency.

Detection of Spin Diffusion Using the Transferred ROE. The contribution of spin diffusion mediated by either ligand or enzyme protons to the TRNOE buildup curves obtained for [2′-²H]tubercidin bound to PNP (Figure 2 and Table 1) was investigated by comparing difference spectra obtained in both the laboratory (TRNOE) and rotating frames (TRROE). As shown in Figure 1C,E, the transferred ROE peaks at τ_{mix} = 200 ms are positive (opposite phase to the inverted or diagonal peak) while the transferred NOE peaks (Figure 1B,D) are negative, as expected for a ligand bound to a macromolecule. Even without careful analysis of buildup curves, one can gain insight into indirect effects by comparing TRNOE and TRROE difference spectra. For example, no TRROE signal was obtained for 2{2′} at 200 ms, while a positive peak was observed for 8{2′}, indicating that the linear TRNOE buildup observed for the former was misleading (Figure 2B). No TRROE signal was observed at any mixing time for 2{2′} or for 2{3′}. Only for the latter was there some indication of a lag in the TRNOE buildup curve. This clearly shows that an efficient spin diffusion pathway is operating between H-2 and sugar protons such as H-2′ and H-3′, presumably mediated by protein spins since there do not appear to be any significant ligand-mediated pathways in most of the geometries examined. Presumably, the lack of any measurable TRROE is a result of strong leakage in the rotating frame and sign changes at each step in the pathway and may also reflect the presence of multiple pathways which produce ROEs of different sign which then tend to cancel each other. Whatever the source of the dissipation of TRROE signals in these cases, it was apparently severe enough to prevent the observation of any sign change, i.e. negative TRROE signals. In fact, a dramatic decrease in the intensity of the protein envelope in TRROE spectra (not acquired in the difference mode) was observed after a spin-lock of as little as 5-ms duration. However, the majority of spin pairs that exhibit TRNOE peaks have corresponding TRROE peaks, including the interactions of greatest interest between H-8 and the sugar protons.

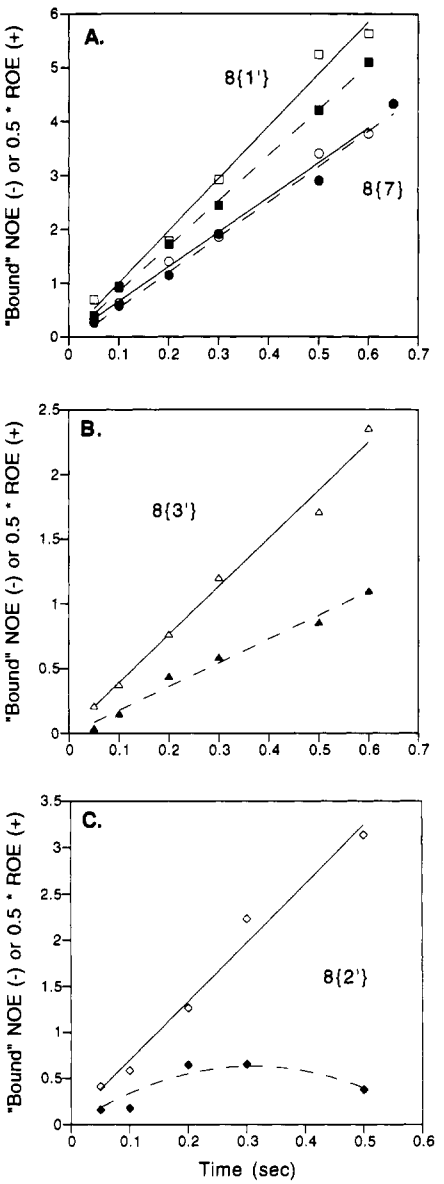

FIGURE 4: Comparison of "bound" NOE and ROE buildup curves for (A and B) [2′-²H]tubercidin/PNP at 20 °C and for (C) tubercidin–PNP at 10 °C (L/E = 40). Open symbols represent NOE data and filled symbols represent ROE data: □, 8{1′}; ○, 8{7}; △, 8{3′}; ◇, 8{2′}. Solid lines are linear fits to the NOE data, and dashed lines are linear (A,B) or quadratic (C) fits to the ROE data.

In order to directly compare quantitatively the TRNOE and TRROE results, "bound" NOE and ROE buildup curves were obtained (Figure 4) by subtracting the contribution from the free ligand using experimentally determined data for the [2′-²H]tubercidin in the absence of enzyme (see Materials and Methods). The bound cross-relaxation rates were measured from the slopes of the linear buildup curves and are given in Table 3. Linear buildup with similar rates for both experiments was observed for 8{7} and 8{1′} in [2′-²H]-tubercidin–PNP, consistent with the interpretation that these interactions arise primarily from direct dipolar interaction of the spin pairs. Thus, from the bound NOE data (σ^{nB}) for 8{1′} and 8{7} and eq 21, one obtains $r_{81'} = 2.53$ Å. Nonlinear buildup curves were observed only for 8{2′} (Figure 4C) and 1′{2′} (data not shown) implying that both of these interactions involve a third spin, presumably H-1′ and H-8, respectively. By fitting the ROE data to a quadratic function, the rate $-0.5\sigma^{rB}$ can be obtained from the linear term, and its similarity to σ^{nB} confirms that a three-spin effect (eqs 14 and 15) is responsible. An average of the distances calculated from

Table 3: Comparison of Results of ROE and NOE Experiments

	tubercidin–PNP (10 °C)				[2′-²H]tubercidin–PNP (20 °C)			
I{S}	σ_B^{nc}	r	$\sigma_B^r/2^d$	r	σ_B^{nc}	r	$\sigma_B^r/2^d$	r
8{7}	−10.6	2.71[a]	7.64	2.71[a]	−6.41	2.71[a]	6.52	2.71[a]
8{1′}	−13.5	2.61	8.75	2.65	−9.67	2.53	8.39	2.60
8{2′}	−6.36	2.95	4.10[b]	3.01				
8{3′}	−3.72	3.23	1.92[b]	3.41	−3.71	2.97	1.83	3.34
1′{2′}	−5.44	3.03	3.08[b]	3.15				

[a] Reference distance in angstroms. [b] From coefficient of linear term from quadratic fit. [c] Bound cross-relaxation rate in laboratory frame (s^{-1}). [d] Bound cross-relaxation rate in rotating-frame divided by 2 (s^{-1}).

$-0.5\sigma^{rB}$ and σ^{nB} for 8{2′} gives $r_{82'}$ = 2.98 Å.

The TRROE buildup rate for 5′,5″{2′} appeared to be slower than that of the TRNOE, but the very rapid dissipation (without sign change) of the ROE signal apparently due to the efficient $T_{1\rho}$ relaxation of the geminal protons prevented any further analysis using the "bound" TRROE curve. However, the strongly quadratic normalized TRNOE buildup (Figure 2C) provides direct evidence for a significant indirect dipolar interaction. In general, more indirect effects were revealed by the TRROE data at 10 °C than at 20 °C. In particular, a greater difference between the TRNOE and TRROE curves for 8{7} and 8{1′} was observed at 10 °C (Table 3). This is presumably due to the greater rates of spin diffusion associated with the longer rotational correlation time at the lower temperature.

In the case of the data for 8{3′} obtained for [2′-²H]-tubercidin–PNP, the ROE buildup appears to be linear (Figure 4B) and there is a significant difference between σ^{nB} and $-0.5\sigma^{rB}$. If spin diffusion is the cause, it presumably is protein mediated due to the removal of the only viable intraligand pathway by use of a 2′-deuterated ligand. In contrast to the above results, which can generally be understood within the context of the equations outlined above, the 8{3′} data are anomalous in that there is a significant difference between the initial slopes of the NOE and the ROE buildup curves, while neither curve exhibits a significant degree of curvature. This result may arise as a consequence of the existence of two bound conformations, as discussed in greater detail below.

Modeling of Single Bound Conformation and Relaxation Matrix Simulations of the TRNOE and TRROE Data. As outlined above, the combined TRNOE and TRROE studies tend to support the intuitive conclusion that the stronger NOE interactions corresponding to the shorter internuclear distances are more significantly dominated by direct dipolar interactions and hence provide the most reliable basis for modeling the bound conformation. Although as noted above, several lines of evidence indicate that a model assuming a single bound conformation is inadequate to fit all of the data, an initial attempt was made to fit the observed TRNOE and TRROE data using a single bound conformation of tubercidin. The $r_{81'}$ and $r_{82'}$ distances obtained as described above were used as constraints (Table 4), and for reasons discussed above, the exocyclic bond of the ribose was initially given a g,g conformation. Energy minimization of tubercidin was conducted by imposing these constraints and using a number of starting conformations for the sugar pucker and a systematic search of glycosidic angles. The only conformation that was not highly strained under these conditions was a *syn*, *3′-exo* structure (Figure 5A). The energy calculated for this conformation was 9.4 kcal above that obtained for minimization without constraints. The glycosidic angle χ (defined as O4′–C1′–N9–C4) is 9.9° and is very different from the value of −112° for the crystal structure of tubercidin, which is characterized by an *anti* conformation about the glycosidic bond (Figure 5B). The *3′-exo* sugar pucker for bound tubercidin is energetically similar to that of the crystal structure, *2′-endo*. However, the exocyclic bond (C4′–C5′) conformation for the crystal structure is g,t. The $r_{83'}$ distance for the bound conformation thus obtained was 5.02 Å.

Table 4: Internuclear Distances (Å) for Bound vs Free Tubericidin

	single bound conformation		multiple bound conformations[c]		tubercidin[d] X-ray:
I{S}	constraints[a]	model[b]	B1	B2	r(Å)
8{7}		2.75	2.71	2.71	2.71
8{1′}	2.53	2.58	2.45	3.83	3.73
8{2′}	2.98	3.08	2.95	3.54	2.15
8{3′}		5.05	4.99	2.69	4.45
1′{2′}		3.02	3.01	2.78	3.01
2′{5′}		4.19	4.22	5.41	3.80
2′{5″}		3.69	3.77	4.82	2.67

[a] Constraints based on TRNOE and TRROE data (Table 3). [b] Model (see Figure 5a) based on energy minimization using these constraints. [c] Major (B1) and minor (B2) conformations (see Figure 8) based on fitting of TRNOE and TRROE data to simulated buildup curves (Figure 7) using eq 22. [d] Crystal structure of tubercidin (Abola & Sundaralingam, 1973) (see Figure 5B).

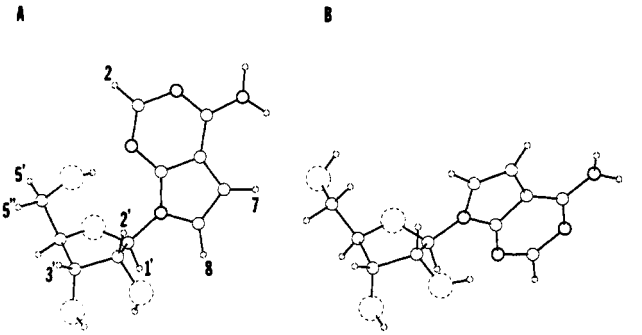

FIGURE 5: Conformation of tubercidin (A) proposed for binding to *E. coli* PNP based on TRNOE data and on the assumption of a single bound conformation and (B) from crystal structure of free ligand.

Relaxation matrix calculations using this bound conformation were then performed using the program "TRNOE" (London et al., 1992) in order to determine how well the observed TRNOE and TRROE data could be simulated when all of the possible cross-relaxation pathways in both the free and bound ligand and the measured rate of exchange between these species are taken into account. The correlation times for bound ligand, τ_{cB}, employed in the relaxation matrix were determined by fitting the 8{7} TRNOE simulations to the corresponding data. The internuclear distances for the bound conformation, r^B_{ij} were based on the distance constraints and molecular modeling described above (Figure 5A). Since the free ligand in solution is a mixture of conformations, the experimental relaxation data obtained in the absence of enzyme, i.e. from σ_{ij} and ρ_{ii} ($1/T_1$ or $1/T_{1\rho}$), were used for $\mathbf{R}_F$. The exchange rates measured at the appropriate temperature were utilized for the reduced rate constant, $k = k_{-1}/p_F$. Note that buildup curves from the data and the simulations will differ from the data in Figure 4 in that observed data are used (i.e. σ^{obs} in eq 20), without a correction for the free ligand or the −2 factor for the TRROE. The data and simulations are, however, normalized using eq 5. The TRROE data are also offset and NOE adjusted with eq 6, while the TRNOE simulations of course do not require such a correction.

Using the 8{7} TRNOE data to set τ_{cB}, both the 8{1′} and 8{7} TRNOE and TRROE data for [2′-²H]tubercidin/PNP at 20 °C (Figure 6A) can be fit fairly well with simulated curves, while the simulations for 8{3′} yield much lower rates than those observed experimentally. For tubercidin–PNP at

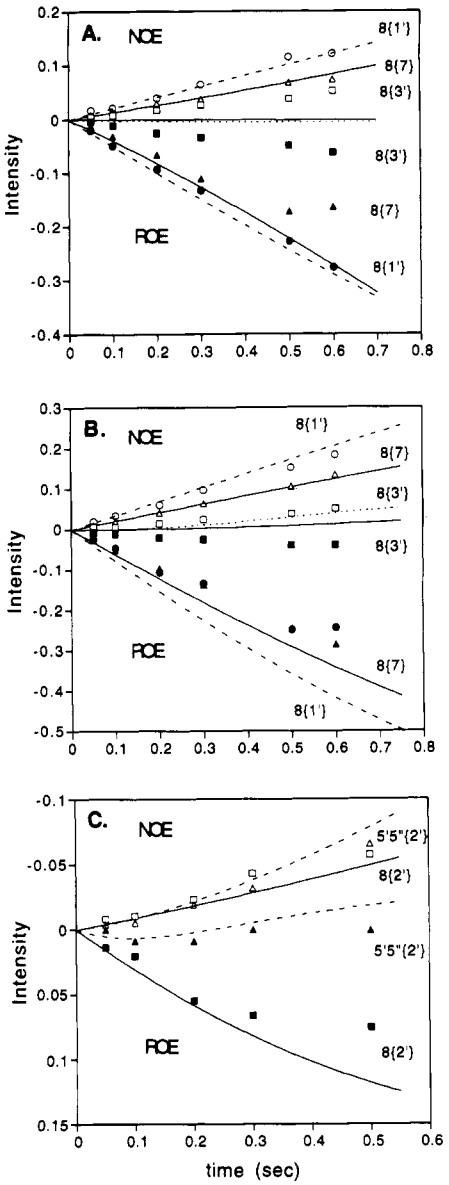

FIGURE 6: Simulation of TRROE and TRNOE buildup curves for (A) [2′-^{2}H]tubercidin–PNP at 20 °C and (B, C) tubercidin–PNP at 10 °C based on a single bound *syn*, 3′-*exo* conformation (Figure 5A). Shown also are the corresponding experimental data, wherein open symbols represent NOE data and filled symbols represent ROE data: (A, B) - - ○ - -, - - ● - -, 8{1′}; –△–, –▲–, 8{7}; –□–, · · ■ · ·, 8{3′}; (C) –□–, –■–, 8{2′}; - - △ - -, - - ▲ - -, 5′5″{2′}. Parameters for simulations: (A) $\tau_C^B = 5 \times 10^{-8}$ s, $k = 2100$ s^{-1}; (B, C) $\tau_C^B = 8.5 \times 10^{-8}$ s; $k_{-1} = 1400$ s^{-1}. Additional parameters: $L/E = 40$; $\rho_B^* = 1$ s^{-1}.

10 °C (Figure 6B,C), a larger τ_{cB} (8.5×10^{-8} s vs 5×10^{-8} s at the higher temperature) was derived from the 8{7} TRNOE, as expected. The TRROE data for 8{7} were also simulated well at this temperature, but the TRROE simulations for 8{1′} and 1′{2′} significantly overestimated the buildup rates, confirming a greater contribution from protein-mediated spin diffusion at 10 °C that was first indicated by the bound ROE curves (Table 3). However, the TRNOE and TRROE data for 8{2′} in tubercidin–PNP (Figure 6C) can be effectively predicted by the simulation, confirming that the indirect effect indicated in Figure 4C is a ligand-mediated effect and that the value for $r_{82'}$ used to model the conformation is reasonable.

Similarly, the TRNOE data for 5′,5″{2′} can be simulated effectively (Figure 6C), and the TRROE data at early mixing times are also close to the calculated curve, again consistent with the conclusion that a ligand-mediated three-spin effect is involved, presumably *via* H-3′, which has strong interactions with both H-2′ and H-5′,5″. This also supports the assignment of the exocyclic bond conformation as g,g. At $\tau_m = 0.3$ s, the experimental TRROE 5′,5″{2′} has disappeared, while a change in sign is predicted by the simulation. This discrepancy appears to arise because the normalized curves can result in large values when the numerator and denominator are both very small, while when the observed NOE or ROE becomes too small to be detected experimentally, no further analysis is possible. We note finally that there is no significant NOE interaction between H-1′ and H-4′. This result is consistent with the *syn*, 3′-*exo* bound conformation in Figure 5A.

However, the simulated curves for 8{3′}, which were not used to obtain a distance constraint, indicate much lower cross-relaxation rates in *both* frames of reference than were observed. This could be caused by protein-mediated spin diffusion, since the matrix does not include any protein spins. This implies, however, that nearly all of the observed TRNOE and TRROE is due to an indirect effect. However, as noted above, multistep ROE transfers through the protein are generally rather weak. An alternative explanation for these data is provided by a model with two bound states, one of which has a much shorter $r_{83'}$ distance. As noted above, the inconsistencies in the $\Delta\delta$ values obtained from variation of the ligand/protein ratio with the values obtained from relaxation data also suggest a model involving an additional bound state.

Modeling Multiple Bound Conformations. Introducing the possibility of a second bound conformation into the calculation requires the introduction of a number of additional parameters. For the present calculations, we have chosen the mathematically simplest approach in which the relaxation matrix for the "bound" state is a weighted average of two possible bound conformations:

$$\mathbf{R}_B = p_{B1}\mathbf{R}_{B1} + p_{B2}\mathbf{R}_{B2} \tag{22}$$

subject to the constraint

$$p_B = p_{B1} + p_{B2} \tag{23}$$

This approximation is equivalent to the usual case of fast exchange between free and bound inhibitors (Landy & Rao, 1989) and will be valid subject to the assumption that the rate of interchange between the two conformers is much larger than all of the auto- and cross-relaxation rates involved in the matrices. Even in the event that the two bound conformers cannot interconvert rapidly while bound to the enzyme, the dissociation rate constants measured are sufficiently high that eq 22 becomes a valid approximation due to dissociation and reassociation of the inhibitor with the enzyme. The use of eq 22 avoids the need to introduce separate parameters for the dissociation rate of each conformer from the enzyme. It is then possible to utilize the same relaxation matrix approach outlined above, with the relaxation matrix for the bound species, $\mathbf{R}_B$, replaced by that defined in eq 22. Even the simple approximation outlined above introduces as additional parameters the two sets of distance matrices corresponding to the two bound states B1 and B2, as well as the ratio of the probabilities for the two states, p_{B1}/p_{B2}.

In calculating the spectral densities for the NOE and ROE interactions, it was assumed that the rotational correlation time for both bound forms is the same. In order to fit the experimental data, the major conformation B1 was initially taken to be similar to the *syn*, 3′-*exo* conformation obtained by assuming only a single bound conformation, while the minor conformation B2 was initially assumed to correspond to an *anti* conformation with a sufficiently short H-8–H-3′ distance to explain the small but significant 8{3′} TRNOE and TRROE

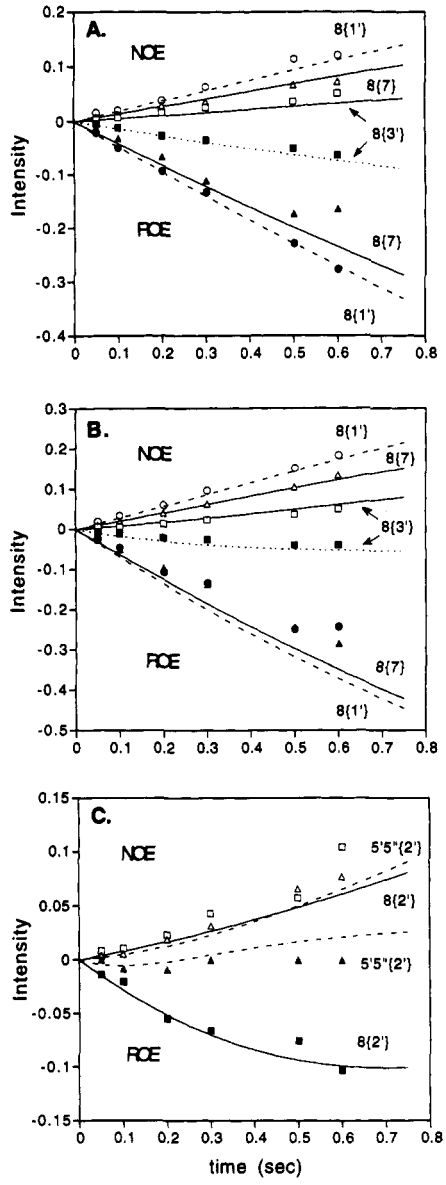

FIGURE 7: Simulation of TRROE and TRNOE buildup curves for a mixture of two bound conformations, B1 (Figure 8A) and B2 (Figure 8B), in a 2:1 ratio. Shown also is the corresponding experimental data. Identification key for graphs and parameters for simulations are the same as for Figure 6, except that $\tau_C^B = 9 \times 10^{-8}$ s for B and C.

signals. Further, unless one of the bound conformations corresponds to an exceedingly large chemical shift for H-2, the ratio p_{B1}/p_{B2} needs to be a small number in order to explain the observed chemical shift data. Additionally, from the standpoint of the NOE results, the use of a ratio far from 1 defeats the strategy of introducing a second bound conformation unless the minor conformation is characterized by unreasonably short internuclear distances. Using a p_{B1}/p_{B2} ratio of either 1 or 2, the three distances $r_{81'}$, $r_{82'}$, and $r_{83'}$ were varied in order to optimize the fit to the TRNOE data obtained at 10 °C for tubercidin. After obtaining a satisfactory fit of the NOE data, distances were varied further to try to optimize the fit of the TRROE data as well, and the process was repeated several times. After fitting the data at 10 °C, the 20 °C data were simulated using the same two bound conformations, but a shorter correlation time. This procedure assumes that the structures and binding ratios characterizing the interaction of tubercidin with PNP are not significantly temperature dependent. A satisfactory agreement between theory and experiment (Figure 7) was obtained using the a 2:1 ratio of the *syn*, 3'-*exo* conformer (B1) relative to an *anti*, 3'-*endo*

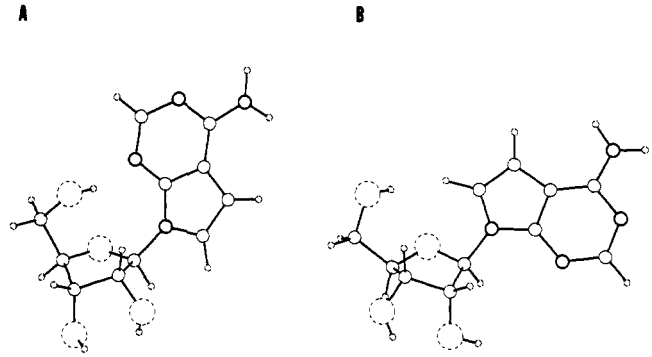

FIGURE 8: Conformations of tubercidin proposed for binding to *E. coli* PNP based on a three-state model: (A) B1 = major bound conformation, (B) B2 = minor bound conformation.

conformer (B2). The agreement between experiment and theory is significantly improved relative to the fits which assume only a single bound conformation (Figure 6), particularly in the case of 8{3'}. The corresponding bound conformations B1 and B2 are shown in Figure 8, and the key distances and other pertinent parameters are given in Table 4. Conformer B1 ($\chi = 9.5°$) is thus very similar to the single conformation deduced above. Conformer B2 has a glycosidic bond conformation ($\chi = -148°$) closer to that of the crystal structure, but with a different sugar pucker. The energy was calculated to be −52.9 kcal for B1 and −56.5 kcal for B2, although these are not necessarily representative of the relative stabilities when bound to the enzyme, due to the energy connected with the binding process.

DISCUSSION

The transferred NOE technique has been used to study the conformation of the complex formed between the inhibitory nucleoside tubercidin and *E. coli* purine nucleoside phosphorylase. Although the broad range of reported applications of this approach suggested that this technique would be ideally suited to this experimental system, several significant difficulties became apparent as these studies progressed: (1) The ligand exchange rate is a critical parameter in this application, since exchange rates which are not sufficiently rapid can result in systematic errors involving underestimation of the cross-relaxation rate between directly interacting spins and overestimation of the cross-relaxation rate between spins for which significant indirect dipolar coupling pathways exist (London et al., 1992). (2) Differentiation between direct and indirect NOE interactions is critical to the success of this technique. Although it has been proposed that the presence of significant indirect relaxation pathways will be reflected in the observation of a significant nonlinearity in the NOE buildup curve, our recent theoretical calculations corresponding to NOESY or selective inversion recovery measurements indicate that this effect is reduced or absent at "intermediate" exchange rates and that, even under conditions of infinitely fast exchange, the nonlinearity may be easy to miss in high molecular weight systems. (3) Although the NOEs of the bound state may dominate the NOEs corresponding to the free state, at high ligand/enzyme ratios the latter may represent significant quantitative perturbations, particularly if critical distances become sufficiently short in the uncomplexed ligand.

Exchange rates which are large enough to lead to a collapse of resonances, i.e. fast exchange on the chemical shift scale, are those most commonly encountered in transferred NOE experiments, and as shown previously (London et al., 1992), determination of these rates is critical to conformational

analysis based on these experiments. However, measurement of these rates cannot readily be achieved using line shape analysis or magnetization transfer techniques as is the case for intermediate or slow exchange processes. In order to approach the first problem noted above, ligand-exchange rates were determined using both CPMG measurements of $1/T_2$ as a function of the pulse rate (Gerig & Stock, 1975) and measurements of $T_{1\rho}$ as a function of the spin-lock field strength. The agreement between the two methods was quite reasonable. These measurements, as well as analysis of relaxation data based on the Swift & Connick equations, yielded values for $\Delta\delta$ of H-2 that conflicted with the values obtained from determinations of chemical shift dependence on L/E ratio. Thus, the assumption of a single bound state is apparently inadequate to describe the physical situation.

In order to deal with the second problem noted above, we have evaluated the use of a transferred ROE or "TRROE" experiment. This represents an extension of an approach which has been reported to be useful for the separation of direct and indirect relaxation pathways in macromolecules (Fejzo et al., 1989; Bauer et al., 1990). Theoretical estimates were obtained based on an expansion of the relaxation matrix as a function of mixing time or using a complete relaxation matrix formalism written in Mathematica which we have recently developed (London et al., 1992). In general, the dominant contributions of the cross-relaxation rates for the bound species is a characteristic of the ROE as well as the NOE experiment, so that a transferred ROE experiment provides a useful way of evaluating the dipolar interactions of macromolecule-complexed ligands. As in the case of nonexchanging systems, indirect ROE interactions between remote nuclei tend to fall off more rapidly than indirect NOE interactions as a consequence of the alternating sign effect, as a consequence of the existence of multiple coupling pathways which may contribute ROEs of different signs, and as a consequence of the leakage of the magnetization into the protein via rotating-frame dipolar interactions. For example, in several cases in which significant NOE interactions were observed, transferred ROE interactions were small or absent. Thus, given the inadequacy of the "lag" in the NOE buildup curve to provide an unequivocal indication of spin diffusion pathways, the TRROE experiment represents an attractive alternative approach to making such a determination.

Additionally, the potential significance of several intraligand dipolar interaction pathways was probed by utilizing [2′-^{2}H]-tubercidin. Removal of protein-mediated spin diffusion has been accomplished in TRNOE studies of binding to lipid membranes by using perdeuterated phospholipids (Wakamatsu et al., 1992), but the perdeuteration of proteins is a more extensive undertaking (LeMaster, 1990).

The third limitation representing quantitative errors due to significant contributions from the NOE or ROE interactions in the uncomplexed ligand was handled by using full relaxation matrix simulations. The calculation utilized a relaxation matrix for the uncomplexed state which was based on direct measurements in the absence of enzyme. The poor fit of some of the NOE interactions, particularly involving H-8–H-3′, was ultimately rationalized in terms of two bound conformations of tubercidin involving a *syn* conformation as the major and an *anti* as a minor bound conformation.

The existence of more than a single bound conformation could be rationalized in principle by nonspecific binding, or by the possibility of two modes of binding to the active site of the enzyme. The ligand competition studies involving 9-deazainosine and tubercidin indicate that reversal of the NOE effects is quantitatively consistent with the inhibition constants for the two nucleosides, which in turn suggests a competition for the active sites of the enzyme. Thus, these studies suggest that the NOE effects are strongly dominated by the binding of tubercidin to the active site(s) of PNP rather than by nonspecifically bound tubercidin. A stronger conclusion could be drawn if a more potent competitive ligand for the bacterial enzyme were available. The possibility of two modes of binding at the active site could indicate similar binding energies for *syn* and *anti* geometries (both of which are present in solution (Evans & Sarma, 1975)) or might arise as a consequence of indirect, allosteric interactions among the six structurally equivalent binding sites of the *E. coli* PNP. However, there is no evidence for either positive or negative cooperativity in kinetic measurements as a function of the concentration of nucleoside substrates (Jensen, 1976), minimizing the likelihood of such interactions. We are thus left with the conclusion that two modes of binding of the tubercidin to a set of equivalent enzyme binding sites can occur, with the *syn*, 3′-*exo* conformation being the predominant bound form. Although this is somewhat unexpected, NMR studies of enzymes and enzyme–substrate complexes in solution increasingly provide evidence for structural heterogeneity. Examples include dihydrofolate reductase (London et al., 1979; Feeney et al., 1983; Birdsall et al., 1989; Huang et al., 1991) and the galactose chemosensory receptor (Luck & Falke, 1991). Transferred NOE studies of $NADP^+$ in the presence of glucose-6-phosphate dehydrogenase have indicated that the nicotinamide moiety binds in both the *syn* and *anti* conformations at a ratio of 70:30 (Gronenborn et al., 1984). Perhaps dead-end complexes involving inactive ligand geometries form more generally than is appreciated and will contribute to the observed TRNOE effect if the ligand is sufficiently constrained in terms of its rotational correlation time. This represents an important caveat for the design and interpretation of transferred NOE studies.

Previous inferences concerning the conformation of nucleosides bound to *E. coli* PNP have been based on the lack of activity or inhibitory potency of conformationally constrained analogs such as aristeromycin and 8-bromoadenosine, which predominantly adopt the *syn* conformation in solution (Doskocil & Holy, 1977). These studies have supported the conclusion that the nucleoside binding site of the *E. coli* enzyme may differ radically from that of the well-characterized human erythrocyte enzyme, requiring an *anti* conformation in the former compared with a *syn* conformation in the latter. The present results indicate the preference of the binding site for a *syn* nucleoside geometry ($\chi = 10°$), which suggests that the inactivity of nucleosides such as 8-bromoadenosine which adopt a *syn* conformation in solution may arise as a consequence of significant steric interactions with the enzyme in the bound state. This illustrates the danger inherent in extrapolating structural data for free ligands to predict enzyme- or receptor-complexed conformations, a problem which is frequently encountered in drug design efforts. Nucleosides bound to the human enzyme favor a high *syn* ($\chi \sim 110°$) conformation (Stoeckler et al., 1986), which is intermediate between a *syn* and *anti* conformation. The conclusion that a *syn* conformation appears to be favored for both the human and the bacterial enzyme may have mechanistic implications. Jordan and Niv (1977b) have shown that, in the acid-catalyzed hydrolysis of purine nucleosides, the fixed *syn* C8-dimethylamino substrates hydrolyze very much faster than the C8-amino and C8-monomethylamino analogs. The present studies indicating that the bacterial enzyme may also favor a *syn* nucleoside geometry provide support for the mechanistic significance of

such a geometry in the enzyme-catalyzed reaction.

SUPPLEMENTARY MATERIAL AVAILABLE

Text describing the detailed determination of the dissociation rate constants on the basis of a Swift and Connick analysis (eqs 8–11), on the basis of $T_{1\rho}$ measurements (eq 12), or using T_2 (CPMG) measurements is available (11 pages). Ordering information is given on any current masthead page.

REFERENCES

Abola, J., & Sundaralingam, M. (1973) *Acta Crystallogr. B29*, 697.

Anderson, N. H., Nguyen, K. T., & Eaton, H. L. (1985) *J. Magn. Reson. 63*, 365.

Avramis, V. I., & Plunkett, W. (1982) *Cancer Res. 421*, 2587–2591.

Banerjee, A., Levy, H. R., Levy, G. C., & Chan, W. W. C. (1985) *Biochemistry 24*, 1593–1598.

Bauer, C. J., Frenkiel, T. A., & Lane, A. N. (1990) *J. Magn. Reson. 87*, 144–152.

Birdsall, B., Feeney, J., Tendler, S. J. B., Hammond, S. J., & Roberts, G. C. K. (1989) *Biochemistry 28*, 2297–2305.

Bothner-By, A. A., Stephens, R. L., Lee, J., Warren, C. D., & Jeanloz, R. W. (1984) *J. Am. Chem. Soc. 106*, 811–813.

Brito, R. M. M., Rudolph, F. B., & Rosevear, P. R. (1991) *Biochemistry 30*, 1461–1469.

Brown, L. R., & Farmer, B. T. (1989) In *Methods in Enzymology* (Oppenheimer, N. J., & James, T. J., Eds.) Vol. 176, pp 199–216, Academic Press, New York.

Carver, J. P., & Richards, R. E. (1972) *J. Magn. Reson. 6*, 89–105.

Clore, G. M., & Gronenborn, A. M. (1982) *J. Magn. Reson. 48*, 402–417.

Clore, G. M., & Gronenborn, A. M. (1983) *J. Magn. Reson. 53*, 423–442.

Cook, W. J., Ealick, S. E., Krenitsky, T. A., Stoeckler, J. D., Helliwell, J. R., & Bugg, C. E. (1985) *J. Biol. Chem. 260*, 12968–12969.

Cook, W. J., Koszalka, G. W., Hall, W. W., Narayana, S. V. L., & Ealick, S. E. (1987) *J. Biol. Chem. 262*, 2852–2853.

Craik, D. J., & Higgins, K. A. (1989) *Annual Report on NMR Spectroscopy*, Vol. 22, pp 61–138, Academic Press, New York.

Davis, D. G. (1987) *J. Am. Chem. Soc. 108*, 3471–3472.

Davis, D. G., Perlman, M. E., & London, R. E. (1994) *J. Magn. Reson.*, in press.

Deverell, C., Morgan, R. E., & Strange, J. H. (1970) *Mol. Phys. 18*, 553–559.

Doskocil, J., & Holy, A. (1977) *Collect. Czech. Chem. Commun. 42*, 370–383.

Ealick, S. E., Rule, S. A., Carter, D. C., Greenhough, T. J., Babu, Y. S., Cook, W. J., Habash, J., Helliwell, J. R., Stoeckler, J. D., Parks, R. E., Jr., Chen, S., & Bugg, C. E. (1990) *J. Biol. Chem. 265*, 1812–1820.

Eaton, H. L., & Anderson, N. H. (1987) *J. Magn. Reson. 74*, 212–225.

Evans, F., & Sarma, R. H. (1975) *Cancer Res. 35*, 1458–1463.

Feeney, J., Birdsall, B., Roberts, G. C. K., & Burgen, A. S. V. (1983) *Biochemistry 22*, 628–633.

Fejzo, J., Zolnai, Z., Macura, S., & Markley, J. L. (1989) *J. Magn. Reson. 82*, 518–528.

Fejzo, J., Zolnai, Z., Macura, S., & Markley, J. L. (1990) *J. Magn. Reson. 88*, 93–110.

Fry, D. C., Kuby, S. A., & Mildvan, A. S. (1987) *Biochemistry 26*, 1645–1655.

Gerig, J. T., & Stock, A. D. (1975) *Org. Magn. Reson. 7*, 249–255.

Giblett, E. G., Ammann, A. J., Wara, D. W., Sandman, R., & Diamond, L. K. (1975) *Lancet 1*, 1010–1013.

Gronenborn, A. M., Clore, G. M., Hobbs, L., & Jeffrey, J. (1984) *Eur. J. Biochem. 145*, 365–371.

Gronenborn, A. M., & Clore, G. M. (1990) *Biochem. Pharmacol. 40*, 115–119.

Hall, W. W., & Krenitsky, T. A. (1990) *Preparative Biochem. 20*, 75–85.

Holy, A. (1976) *Collect. Czech. Chem. Commun. 41*, 2096–2109.

Huang, F.-Y., Yang, Q.-X., & Huang, T.-H. (1991) *FEBS Lett. 289*, 231–234.

Ikehara, M., Uesugi, S., & Yoshida, K. (1972) *Biochemistry, 11*, 830–836.

Jen, J. (1978) *J. Magn. Reson. 30*, 111–128.

Jensen, K. F. (1976) *Eur. J. Biochem. 61*, 377–386.

Jensen, K. F., & Nygaard, P. (1975) *Eur. J. Biochem. 51*, 253–265.

Jordan, F., & Niv, H. (1977a) *Biochim. Biophys. Acta 476*, 265–271.

Jordan, F., & Niv, H. (1977b) *Nucleic Acids Res. 4*, 697–709.

Kohda, D., Kawai, G., Yokoyama, S., Kawakami, M., Mizushima, S., & Miyazawa, T. (1987) *Biochemistry 26*, 6531–6538.

Krenitsky, T. A., Koszalka, G. W., & Tuttle, J. V. (1981) *Biochemistry 20*, 3615–3621.

Landy, S. B., & Rao, B. D. N. (1989) *J. Magn. Reson. 81*, 371–377.

Laszlo, P. (1979) *Prog. NMR Spectrosc. 13*, 257–270.

LeMaster, D. M. (1990) *Q. Rev. Biophys. 23*, 133–174.

Lim, M.-I., Ren, W.-Y., Otter, B. A., & Klein, R. S. (1983) *J. Org. Chem. 48*, 780–788.

London, R. E., Groff, J. P., & Blakley, R. L. (1979) *Biochem. Biophys. Res. Commun. 86*, 779–786.

London, R. E., Perlman, M. E., & Davis, D. G. (1992) *J. Magn. Reson. 97*, 79–98.

Luck, L. A. & Falke, J. J. (1991) *Biochemistry 30*, 4248–4256.

Macura, S., Farmer, B. T., & Brown, L. R. (1986) *J. Magn. Reson. 70*, 493.

Miles, D. W., Townsend, L. B., Robins, M. J., Robins, R. K., Inskeep, W. H., & Eyring, H. (1970), *J. Am. Chem. Soc. 93*, 1600–1608.

Neuhaus, D., & Williamson, M. P. (1989) *The Nuclear Overhauser Effect in Structural and Conformational Analysis*, pp 312–327, VCH Publishers, Inc., New York.

Perlman, M. E. (1993) *Nucleosides Nucleotides, 12*, 73–82.

Pike, J. E., Slechta, L., & Wiley, P. F. (1964) *J. Heterocycl. Chem. 1*, 159–161.

Stock, A. D. (1974) Ph.D. Thesis, University of California—Santa Barbara, Santa Barbara, CA.

Stoeckler, J. D., Ealick, S. E. Bugg, C. E., & Parks, R. E. (1986) *Fed. Proc. 45*, 2773–2778.

Swift, T. J., & Connick, R. E. (1962) *J. Chem. Phys. 37*, 307–320.

Sykes, B. D., & Scott, M. D. (1972) *Ann. Rev. Biophys. Bioeng. 1*, 27–50.

Tuttle, J. V., & Krenitsky, T. A. (1984) *J. Biol. Chem. 259*, 4065–4069.

Wakamatsu, K., Okada, A., Miyazawa, T., Ohya, M., & Higashijima, T. (1992) *Biochemistry 31*, 5654–5660.

Wennerstrom, H. (1972) *Mol. Phys. 24*, 69–80.